

# Nanoparticle Electric Propulsion for Space Exploration

Thomas M. Liu<sup>1</sup>, Louis D. Musinski<sup>2</sup>, Prashant R. Patel<sup>3</sup>,  
Alec D. Gallimore<sup>4</sup>, Brian E. Gilchrist<sup>5</sup>, Michael Keidar<sup>6</sup>

<sup>1,3,4,6</sup>*Aerospace Engineering*, <sup>2,5</sup>*Electrical Engineering*, <sup>5</sup>*Space Systems*, and <sup>4</sup>*Applied Physics*,  
*University of Michigan, Ann Arbor, MI 48109, USA*  
<sup>1</sup>720-984-4481, liutm@umich.edu

**Abstract.** A new electrostatic thruster technology is under development at the University of Michigan using nanoparticles as propellant with micro- and nano-electromechanical systems. Termed the nanoparticle field extraction thruster (nanoFET), this highly integrated propulsion concept is a high efficiency, variable specific impulse engine type that can be readily scalable for a large range of future space science and exploration missions.

**Keywords:** electric propulsion, MEMS, nanoparticles, variable specific impulse, scalable space systems

**PACS:** 52.75.Di, 73.63.-b, 77.84.Nh, 81.07.-b, 85.85.+j

## INTRODUCTION

Recently, electric propulsion (EP) has been successfully demonstrated as primary propulsion systems for NASA's Deep Space 1 (Rayman *et al.*, 2000), Japan's HAYABUSA (Kuninaka *et al.*, 2006), and ESA's SMART-1 missions (Koppel *et al.*, 2005). By significantly reducing the required propellant mass compared to conventional chemical rockets, EP thrusters can be used to increase the payload capacity or decrease the launch mass. In addition, more orbital maneuvers and longer orbital maintenance durations can be achieved with EP systems for a given propellant mass, thus extending the mission's useful lifetime. With these advantages, EP systems are promising technologies for future solar system science and exploration missions.

A novel concept to advance EP technology is currently under development at the University of Michigan to enhance existing as well as to enable future, more ambitious missions. Named the nanoparticle field extraction thruster (nanoFET), this concept uses highly scalable MEMS/NEMS (micro/nano-electromechanical systems) technologies applied to nanoparticle electric propulsion (Musinski *et al.*, 2005). A series of stacked gates consisting of alternating, micron-scale thick conductive and dielectric layers is used to provide the electric fields necessary to electrostatically charge and accelerate conductive nanoparticles for thrust (Liu *et al.*, 2006a). By using nanoparticles of well characterized dimensions and charge states, nanoFET achieves great flexibility in controlling the propellant's specific charge to tune thruster performance. Millions of miniaturized, integrated nanoFET emitters can be grouped into functional arrays usable from micro- to high-power spacecraft and readily scaled to systems in between.

This paper describes the nanoFET concept and the different thruster configurations currently under development. The paper then discusses the functional and operational advantages offered by nanoFET over other EP technologies for future solar system science and exploration missions.

## NANOFET CONFIGURATIONS

In nanoFET, the nanoparticle propellant, whether stored or manufactured *in situ*, must be transported to the emission sites beneath the electrically biased MEMS gates. At these emission sites, the particles would be charged and accelerated by the imposed electric fields to generate propulsive thrust. Configurations for nanoFET using a

recirculating, microfluidic feed system to transport the nanoparticles are described below. Depending on if the liquid is dielectric or conductive, important differences exist in the particle charging process, transport to the liquid surface, and extraction from the liquid surface. While liquid-less transport options for the nanoparticles may be possible, such concepts are less developed than the liquid transport schemes. Figure 1 shows the cross-sectional view of individual nanoFET emitters of the dielectric and conductive liquid configurations. In either case, the liquid must not be volatile to avoid excessive fluid loss to the space environment, and the liquid's wetting characteristics with respect to the gate materials must be matched such that a consistent liquid-vacuum interface is maintained. By using stacked gate structures, large acceleration potentials may be applied, decoupled from the electric potential needed to extract the particles from the liquid, without exceeding the breakdown strength of the separate dielectric layers. Preliminary charged particle trajectory simulations also suggest that beam collimation is improved with a stacked gate design, resulting in improved thruster efficiency and lifetime.

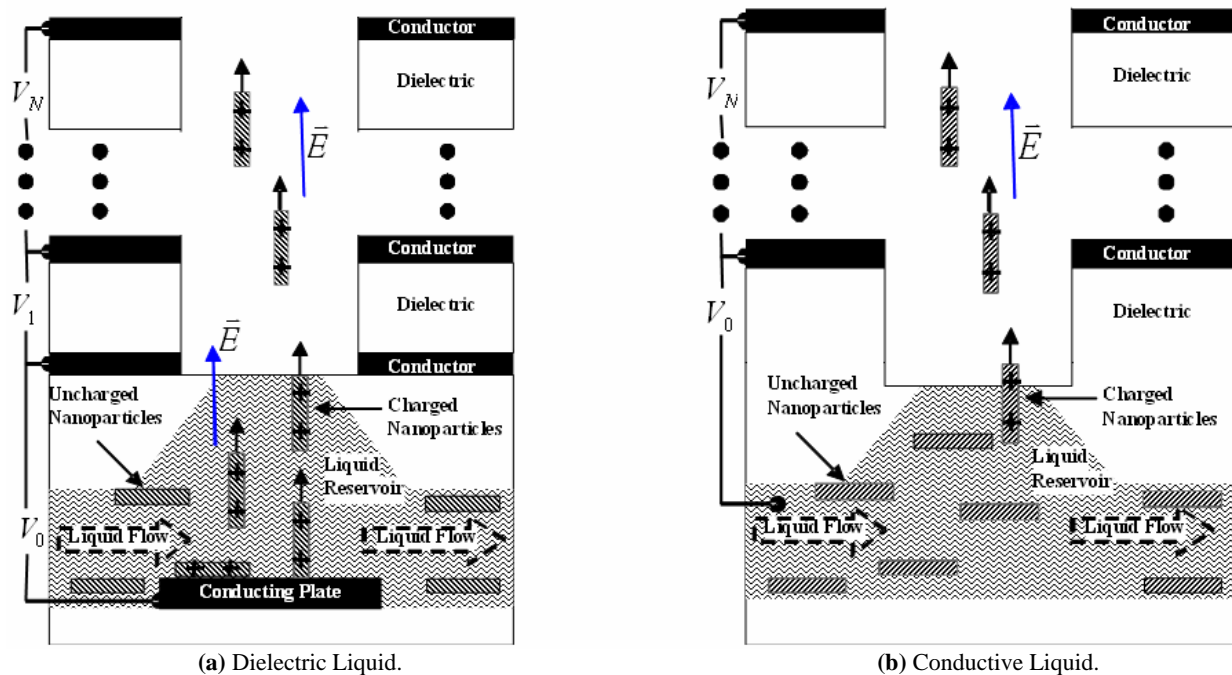


FIGURE 1. NanoFET Emitter Configurations with Liquid Feed System.

### Dielectric Liquid Configuration

A potential bias is applied between the stacked gate structure and the charging plate submerged within the dielectric liquid. As a result, electric fields are generated both within and above the liquid. Conductive particles delivered to the liquid reservoir come in contact with the conducting plate and become charged; if the particles are cylindrical, the acquired charge is directly proportional to the liquid electric field according to Equation (1) (Félici, 1966). When a particle becomes sufficiently charged, it lifts off the charging electrode and is transported to the liquid surface by the imposed electric field. If the particle has sufficient energy to break through the liquid surface, field focusing extracts the particle from the liquid. The particle is then accelerated through the gate structure and ejected to produce thrust. Proof-of-concept tests at larger size scales have already demonstrated the feasibility of this configuration, with particle charging, transport, extraction, and acceleration prior to the onset of liquid surface instabilities (Musinski *et al.*, 2006).

$$q_0 = \pi \frac{l^2}{\ln\left(\frac{2l}{r}\right) - 1} \epsilon_l E_l. \quad (1)$$

## Conductive Liquid Configuration

For conductive liquids, a potential bias applied between the stacked gate structure and the liquid reservoir results in electric fields above the liquid only. Once delivered to the liquid reservoir, conductive particles cannot be charged within the liquid, since no electric field exists within the liquid reservoir. To become charged, the particles must reach the liquid surface. This transport can be accomplished through thermal motion or convective mixing. Particles at the liquid surface become charged in the presence of the vacuum electric field in the same manner as particles become charged in the dielectric configuration in the presence of the liquid electric field. Field focusing then extracts the particle from the liquid, resulting in particle acceleration through the gate structure and ejection from the thruster. Proof-of-concept tests at larger size scales are currently in progress.

## Configuration Considerations

For the dielectric liquid configuration, the specific charge just prior to extraction from the liquid scales approximately as Equation (2) for cylindrical particles of long aspect ratios. To obtain a high particle specific charge, which would require less acceleration potential for a desired thruster specific impulse (Isp), particles of low mass densities, large lengths, and large aspect ratios are desired.

$$\frac{q}{m} \propto \frac{\epsilon_i E_i}{\rho_p l} \frac{A^2}{\ln(4A)} \exp\left[-\frac{\mu_i \sigma_i}{\epsilon_i^2 E_i^2} \frac{\ln(4A)}{\ln A} \frac{d_i}{l}\right], \quad A \equiv \frac{l}{2r} \gg 1. \quad (2)$$

Charged particles within the dielectric liquid experience viscous drag and charge loss due to the finite electrical conductivity of the liquid. These energy losses prior to particle extraction from the liquid surface are the principal sources of inefficiency in the dielectric liquid nanoFET configuration. As seen in Equation (2), these inefficiencies can be reduced by using a liquid of both low viscosity and low electrical conductivity. In addition, the associated energy loss to the liquid can be mitigated by decreasing the time a particle spends traversing the liquid layer; thus, a shallower liquid layer, as long as it still submerses a particle during the charging process, is desired.

The dielectric liquid configuration is simpler to implement, since the nanoparticles are electrostatically transported to the liquid surface by the same electric field used to charge them. In contrast, the conductive liquid configuration requires an alternative means of transporting the nanoparticles to the liquid surface, or the liquid in the reservoir must be shallow enough to expose the nanoparticles. However, the conductive liquid configuration does offer potential advantages. First, charge loss may not be a concern since the particle is charged at the liquid surface. Second, whereas the dielectric liquid configuration has its maximum allowable current density reduced by the presence of viscous drag on the charged particles as they traverse the liquid reservoir (Liu *et al.*, 2006b), this issue is not present for the conductive liquid case. Consequently, the conductive liquid configuration can operate much closer to the vacuum space charge limit, with correspondingly higher thrust, at modest electric field strengths.

With liquid-less configurations, if the issue of transporting particles from their storage or *in situ* manufacturing sites to the emission zones can be resolved, then significant advantages over the liquid configurations can be obtained. Such a liquid-less configuration would likely lower the thruster specific mass, since no liquid is present. Potential liquid loss due to particle wetting would no longer be a concern. Also, a liquid-less configuration does not have to worry about exciting electrohydrodynamic waves. In the liquid nanoFET configurations, failure to avoid these liquid surface instabilities may lead to Taylor cone formation and the generation of colloids, whose size and charge variability would offset the precise thrust controllability afforded by the nanoparticles.

## NANOFET SYSTEM ADVANTAGES

For future solar system science and exploration missions, significant functional and operational advantages may be achieved with nanoFET over other EP technologies. These advantages include the ability to afford a broader set of missions and mission phases with a single engine type, the decoupling of propulsion system design from spacecraft

design, and other mission enhancing and enabling features such as the potential for improved operational life and lower thruster specific mass.

### Mission Flexibility with Single Engine Type

The ability of nanoFET to continuously tune propulsion characteristics via different nanoparticle dimensions and charge states permits a large range of operational  $I_{sp}$ , shown in Equation (3) to be directly proportional to the square root of the propellant particles' specific charge. By electrostatically charging rather than ionizing the propellant, nanoFET is able to achieve high thruster internal efficiencies, expressed in Equation (4) as the ratio between the thruster's jet power and the propulsion system's input power. Thus, the internal efficiency takes into account the power processing unit (PPU) efficiency. When used as a variable- $I_{sp}$  engine, nanoFET can accomplish a broad class of missions and mission phases.

$$I_{sp} = \frac{1}{g_0} \sqrt{2V \frac{q}{m}}. \quad (3)$$

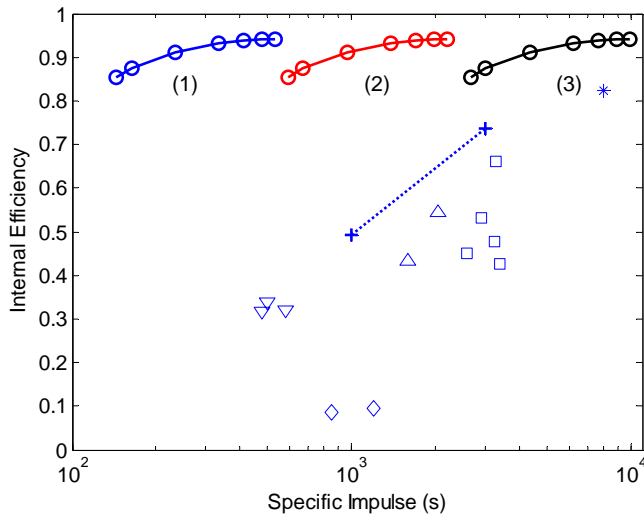
$$\eta_{int} = \frac{\frac{1}{2} g_0 T I_{sp}}{P_{in}}. \quad (4)$$

#### *Large $I_{sp}$ Range at High Efficiencies*

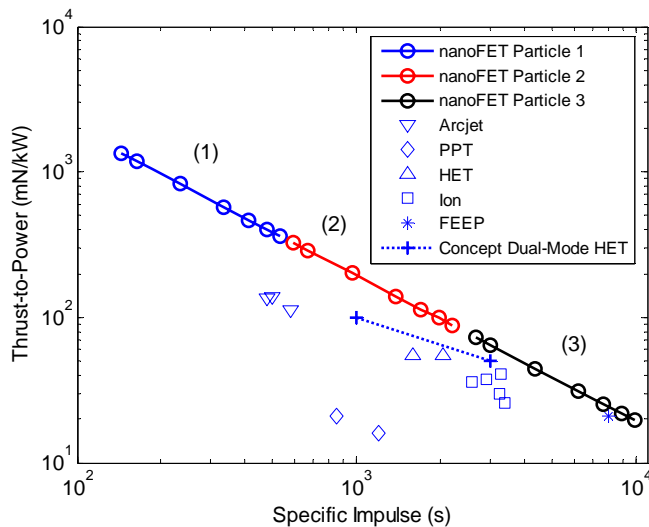
Figure 2 shows the projected nanoFET performance for the dielectric liquid configuration using silicone oil as the liquid compared with other state-of-the-art EP systems (Wertz and Larson, 1999). An assumed PPU efficiency of 0.95 for the nanoFET system results in internal efficiencies over 85% for an  $I_{sp}$  range of 100 to 10,000 seconds using three different types of carbon nanotubes. 800-V to 10-kV accelerating potentials are used for carbon nanotubes of (1) 5-nm diameter and 100-nm length, (2) 1-nm diameter and 100-nm length, and (3) 1-nm diameter and 3.5- $\mu$ m length. Emitter inefficiencies are principally due to viscous drag and charge loss to the liquid, and efficiency losses associated with particle impingement on the gate structures and beam divergence are expected to be no worse than those of existing EP systems. From Equation (4), such high internal efficiencies associated with nanoFET translate to thrust-to-power ratios, particularly at low  $I_{sp}$ , that are greater than state-of-the-art EP thrusters. For applications that do not demand the entire 100 to 10,000 seconds  $I_{sp}$  range, a wide  $I_{sp}$  range can still be achieved with a single nanoparticle type, which simplifies the overall system integration. For example, a dielectric liquid configuration can potentially use carbon nanotubes with 1-nm diameter and 400-nm length and acceleration potentials ranging from 400 V to 10 kV to span an  $I_{sp}$  range of 800 to 4,000 seconds at over 85% internal efficiency.

No other state-of-the-art ion or hall thrusters in Figure 2 are designed to span such a large  $I_{sp}$  range at high efficiencies and high thrust-to-power ratios. For low- $I_{sp}$ , high thrust-to-power maneuvers, nanoFET would outperform arcjets by achieving greater thrust for the same power. At high  $I_{sp}$ , nanoFET's projected performance is comparable to field emission electric propulsion (FEEP) thrusters operating in ion mode. However, in the low- $I_{sp}$  regime, FEEP thrusters must operate in colloid mode, resulting in a dispersion in the specific charge distribution and less thrust controllability compared to nanoparticles with precise charge states.

The significance of such a wide  $I_{sp}$  range at high efficiencies for nanoFET is that it provides mission designers with tremendous flexibility. Consider a robotic probe or a freighter vehicle to a planetary body. During interplanetary cruise, nanoFET would operate in a high- $I_{sp}$  mode to minimize the propellant cost. Once within the planetary body's gravity well, nanoFET could switch to a low- $I_{sp}$ , high thrust-to-power mode to provide greater thrust capability. This flexibility also provides a wider margin for both robotic and crewed missions to accommodate off-nominal and abort scenarios, adjust the flight time, and perform dynamic retasking to take advantage of in-flight opportunities. To achieve comparable capabilities with other EP systems across the entire  $I_{sp}$  range, multiple engine types would have to be used, which tends to increase the mass of the propulsion system while complicating spacecraft integration and design (Oleson, 2000).



(a) Internal Efficiency for Large Isp Range.



(b) Thrust-to-Power for Large Isp Range.

**FIGURE 2.** NanoFET’s Performance Compared with State-of-the-Art Electric Propulsion Systems.

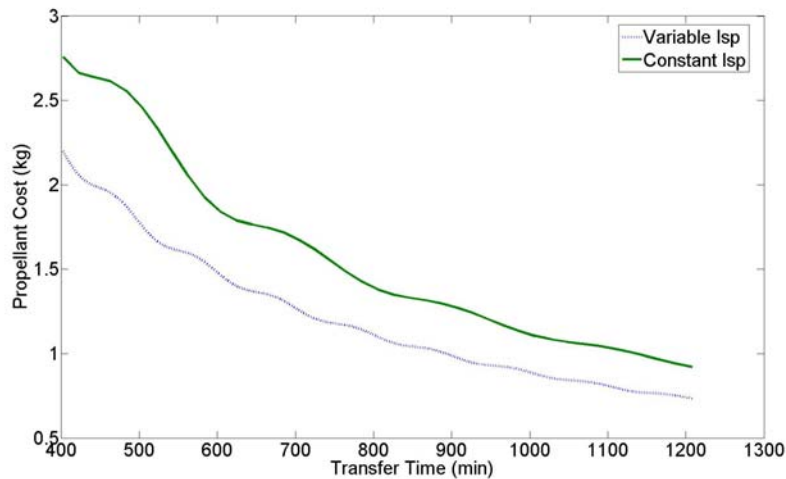
engine is chosen for a spacecraft, then it will not be propellant optimal for the unknown future maneuvers, since the Isp was optimized without taking into account the unknown maneuvers. If a variable-Isp engine is used, then the Isp can be varied over time to ensure that the orbit change utilizes the minimum amount of propellant. Using a variable-Isp engine would also allow a time-propellant trade to be conducted. If the propellant amount is considered fixed, the minimum time in which a maneuver can be accomplished will be lower for the variable-Isp engine, since it can deliver the necessary acceleration when it can be best utilized simply by adjusting the Isp (Patel, Scheeres, and Gallimore, 2006).

As a simple example of the benefits of a variable-Isp engine, consider a spacecraft orbiting the Earth with an initial mass of 1,000 kg that needs to be raised from 5,000-km to 5,100-km altitude. Using a 5-kW jet power variable-Isp nanoFET engine, a distinctive propellant-time trade can be conducted to help the spacecraft operator best determine how to conduct the maneuver. This trade is shown in Figure 3 along with the range of Isp utilized for each transfer time. Note that for a desired transfer time, the variable-Isp engine is more propellant efficient than the optimum constant-Isp engine. For maneuvers that are not time critical, the operator can use long time maneuvers, which

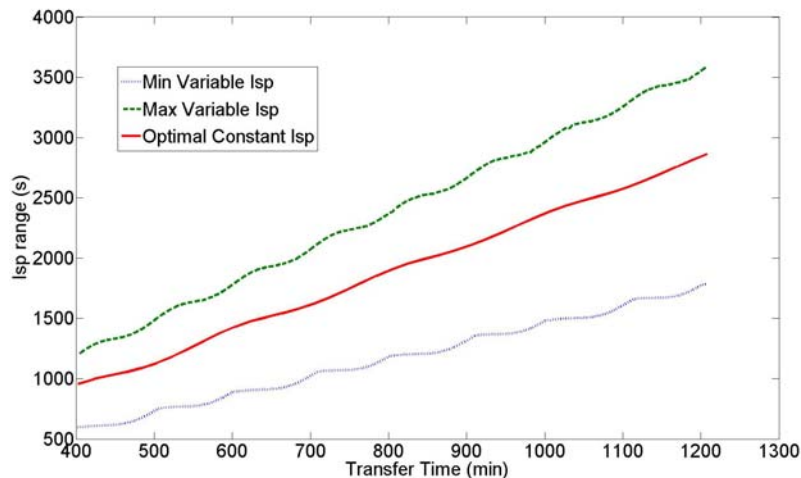
The flexibility of adjusting the specific charge and the acceleration potential in the nanoFET system means that it is a variable-Isp engine. From a system analysis point of view, a variable-Isp engine is akin to having infinitely many constant-Isp engines in one. A constant-Isp engine’s performance is a subset of the performance available to a variable-Isp engine, which can optimize the Isp at each point in time to minimize the propellant use. For this reason, a variable-Isp engine will always consume less propellant than a constant-Isp engine. In certain cases, dual-mode constant-Isp engines can approach the minimal propellant cost given by variable-Isp systems (Casalino and Colasurdo, 2004). The caveat to achieving the near equivalent performance requires that the dual-mode constant-Isp engine be designed specifically for the mission. This requirement is a significant problem because designing, testing, and validating an engine can take years (Sovey *et al.*, 1997). Also, in order to optimize the engine, the mission profile would have to be known before development began. If during development the thrust profile changes due to a delayed launch or to funding or technical decisions, then the engine would become non-optimal. A variable-Isp engine eliminates the need for optimizing engines specifically for missions because the thrust profile can be made propellant optimal without redesigning the engine.

For missions that require unplanned or unknown maneuvers, such as for remote sensing or observation missions, variable-Isp engines are beneficial. If a constant-Isp

would conserve propellant for mission critical situations in which timing may be very important. A variable-Isp engine changes the problem from figuring out how to best estimate future mission needs to one of determining how critical each operation is, thus allowing the user to best determine how to utilize the present propellant budget.



(a) Minimum Propellant Cost.



(b) Bounds of Isp Range to Achieve a Desired Transfer Time.

**FIGURE 3.** Earth Orbit Transfer Comparison for Variable-Isp NanoFET and Optimum Constant-Isp Engine.

## Decoupling of Propulsion System from Spacecraft Design

The use of MEMS technology enables a highly integrated, “flat panel” nanoFET design that incorporates power processing as well as nanoparticle manufacture, storage, feed, extraction, and acceleration. Such compact, “plug-and-play” design simplifies propulsion system integration and lowers the thruster specific mass. Because different regions of nanoFET can operate in a bipolar manner to emit particles of opposite polarity, neutralizer requirements are simplified as nanoFET is a self-neutralizing thruster.

Figure 4 shows the nanoFET system at different characteristic size scales, from individual emitter elements up to a prototype array fabricated on a silicon wafer. Depending on the mission requirements, the nanoFET emitter array may be straightforwardly scaled to span a broad power range, from less than a watt to tens of kilowatts or more. This scalability means that nanoFET can potentially be used for a diverse set of missions, ranging from formations

of microsattellites to flagship-type science missions. By leveraging the use of a single engine type across all these missions, time and cost for propulsion system development, testing, and qualification would be reduced.

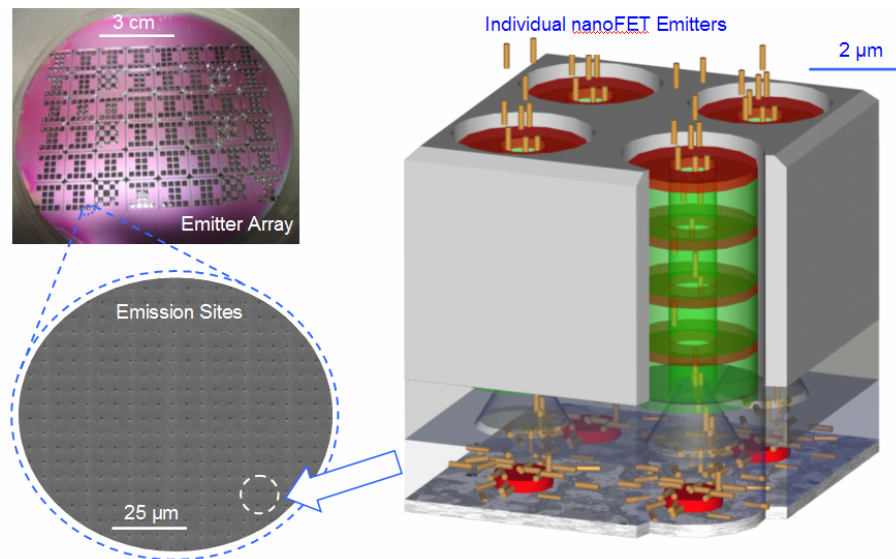


**FIGURE 4.** Nanoparticle Field Extraction Thruster Characteristic Size Scales.

### Other Mission Enhancing and Enabling Features

Having EP systems with long operational lifetimes is important for future missions that require continuous propulsion capability for tens to hundreds of kilo-hours. The nanoFET concept's operational lifetime is not driven by the primary life-limiting factors of state-of-the-art EP systems. Since the nanoparticles are charged electrostatically rather than ionized as in ion or Hall thrusters, greater reliability and efficiency can be achieved. Without the need to ionize propellant, nanoFET does not experience charge exchange (CEX) collisions between high energy charged and slow moving neutral particles. These CEX collisions result in low energy charged particles that are the primary surface erosion mechanism for ion thrusters (Katz *et al.*, 2005). Since hollow cathodes are not needed for ionization or neutralization on nanoFET, another principal lifetime limiter for other EP systems is eliminated. The potential for longer life means that fewer redundant thruster elements are needed compared to conventional EP thrusters, thus resulting in decreased thruster specific mass.

This lower thruster specific mass means that for a given spacecraft mass, more mass can be devoted to payload. Lower thruster specific mass may also be obtained by nanoFET's potential to operate at higher thrust densities than conventional EP thrusters. Whereas state-of-the-art ion thrusters operate substantially below the space charge limit to ensure proper ion optics operation, nanoFET should be able to operate much closer to the space charge limit since the charges are contained in a fewer number of particles.

### CONCLUSION

The nanoFET concept is an attractive propulsion system for future space science and exploration missions. Being a variable-Isp engine that is geometrically scalable, nanoFET potentially has the performance and integration flexibility to be employed on a diverse set of missions. In addition, the advantages offered by nanoFET's potential for high efficiencies, lower thruster specific mass, and longer operational lifetimes are both mission enhancing and enabling.

## NOMENCLATURE

$A$	= cylindrical particle aspect ratio	$q_0$	= initial particle charge (C)
$d_l$	= liquid layer thickness (m)	$r$	= particle radius (m)
$E_l$	= liquid electric field (V/m)	$T$	= thrust (N)
$g_0$	= gravitational acceleration at Earth's surface (m/s <sup>2</sup> )	$V$	= acceleration potential (V)
$I_{sp}$	= specific impulse (s)	$\epsilon_l$	= permittivity of liquid (F/m)
$l$	= cylindrical particle length (m)	$\eta_{int}$	= thruster internal efficiency
$m$	= particle mass (kg)	$\mu_l$	= dynamic viscosity coefficient of liquid (Pa·s)
$P_{in}$	= input power to propulsion system (W)	$\rho_p$	= particle mass density (kg/m <sup>3</sup> )
$q$	= particle charge (C)	$\sigma_l$	= liquid electrical conductivity (S/m)

## ACKNOWLEDGMENTS

This project is funded by a Phase 2 grant (NAS5-03110) from the NASA Institute for Advanced Concepts and supported by a National Defense Science and Engineering Graduate Fellowship (Liu) and a NASA Graduate Student Researchers Program fellowship (Patel). Thanks to Matthew Forsyth at the University of Michigan (UM) for helping to construct the proof-of-concept experimental setups. Special thanks to Bailo Ngom from the UM Plasmadynamics and Electric Propulsion Laboratory for his help with Figure 4.

## REFERENCES

- Casalino, L. and Colasurdo, G., "Optimization of Variable-Specific-Impulse Interplanetary Trajectories," *Journal of Guidance, Control, and Dynamics* **27** (4), 678-684 (2004).
- Félici, N.-J., "Forces et charges de petits objets en contact avec une électrode affectée d'un champ électrique," *Revue Générale de l'Électricité* **75**, 1145-60 (1966).
- Katz, I., Mikellides, I., Wirz, R., Anderson, J., and Goebel, D., "Ion Thruster Life Models," in proceedings of *41st AIAA/ASME/SAE/ASEE Joint Propulsion Conference (2005)*, AIAA, Reston, VA, 2005, Paper No. AIAA-2005-4256.
- Koppel, C., Marchandise, F., Prioul, M., Estublier, D., and Darnon, F., "The SMART-1 Electric Propulsion Subsystem around the Moon: In Flight Experience," in proceedings of *41st AIAA/ASME/SAE/ASEE Joint Propulsion Conference (2005)*, AIAA, Reston, VA, 2005, Paper No. AIAA-2005-3671.
- Kuninaka, H., Nishiyama, K., Funaki, I., Yamada, T., Shimizu, Y., and Kawaguchi, J., "Powered Flight of HAYABUSA in Deep Space," proceedings of *42nd AIAA/ASME/SAE/ASEE Joint Propulsion Conference (2006)*, AIAA, Reston, VA, 2006, Paper No. AIAA-2006-4318.
- Liu, T., Morris, D., Cionca, C., Gallimore, A., Gilchrist, B., and Clarke, R., "MEMS Gate Structures for Electric Propulsion Applications," in proceedings of *42nd AIAA/ASME/SAE/ASEE Joint Propulsion Conference (2006)*, AIAA, Reston, VA, 2006a, Paper No. AIAA-2006-5011.
- Liu, T., Keidar, M., Musinski, L., Gallimore, A., and Gilchrist, B., "Theoretical Aspects of Nanoparticle Electric Propulsion," in the proceedings of *42nd AIAA/ASME/SAE/ASEE Joint Propulsion Conference (2006)*, AIAA, Reston, VA, 2006b, Paper No. AIAA-2006-4335.
- Musinski, L., Liu, T., Gilchrist, B., Gallimore, A., and Keidar, M., "Scalable Flat-Panel Nano-Particle MEMS/NEMS Thruster," in proceedings of *29th International Electric Propulsion Conference (2005)*, IEPC, Princeton, NJ, 2005, IEPC-2005-176.
- Musinski, L., Liu, T., Gilchrist, B., Gallimore, A., and Keidar, M., "Nanoparticle Electric Propulsion: Experimental Results," in the proceedings of *42nd AIAA/ASME/SAE/ASEE Joint Propulsion Conference (2006)*, AIAA, Reston, VA, 2006, Paper No. AIAA-2006-4803.
- Oleson, S., *Mission Advantages of Constant Power, Variable Isp Electrostatic Thrusters*, NASA/TM 2000-210477, NASA Glenn Research Center, Cleveland, OH, 2000.
- Patel, P., Scheeres, D., and Gallimore, A., "Maximizing Payload Mass Fractions of Spacecraft for Interplanetary Electric Propulsion Missions," *Journal of Spacecraft and Rockets* **43** (4), 822-7 (2006).
- Rayman, M., Varghese, P., Lehman, D., and Livesay, L., "Results from the Deep Space 1 Technology Validation Mission," *Acta Astronautica* **47**, 475 (2000).
- Sovey, J., et al., *Development of an Ion Thruster and Power Processor for New Millennium's Deep Space 1 Mission*, NASA/TM 113129, NASA Lewis Research Center, Cleveland, OH, 1997.
- Wertz, J. and Larson, W., *Space Mission Analysis and Design*, Microcosm Press, El Segundo, CA, 1999, p. 703.